Molecular Crystals and Liquid Crystals

ISSN: 1542-1406 (Print) 1563-5287 (Online) Journal homepage: https://www.tandfonline.com/loi/gmcl20

Controlling the Aspect Ratio of Silver Nanowires by Variation of Polyvinylpyrrolidone/$AgNO_3$ Contents

Bona Kim , Hyun Ho Park , Youngeun Choi , Do Hyeong Kim , Young Soo Yun & Hyoung-Joon Jin

To cite this article: Bona Kim , Hyun Ho Park , Youngeun Choi , Do Hyeong Kim , Young Soo Yun & Hyoung-Joon Jin (2012) Controlling the Aspect Ratio of Silver Nanowires by Variation of Polyvinylpyrrolidone/$AgNO_3$ Contents, Molecular Crystals and Liquid Crystals, 566:1, 112-119, DOI: 10.1080/15421406.2012.701858

To link to this article: https://doi.org/10.1080/15421406.2012.701858

Published online: 12 Sep 2012.

Mol. Cryst. Liq. Cryst., Vol. 566: pp. 112–119, 2012

ISSN: 1542-1406 print/1563-5287 online
DOI: 10.1080/15421406.2012.701858

Taylor & Francis
Taylor & Francis Group

Controlling the Aspect Ratio of Silver Nanowires by Variation of Polyvinylpyrrolidone/$AgNO_3$ Contents

BONA KIM, HYUN HO PARK, YOUNGEUN CHOI, DO HYEONG KIM, YOUNG SOO YUN, AND HYOUNG-JOON JIN*

Department of Polymer Science and Engineering, Inha University, Incheon 402-751, Korea

The effects of different molar ratios between polyvinylpyrrolidone (PVP) and $AgNO_3$ on the length of silver nanowires and of the aspect ratio of the silver nanowires on the electrical percolation threshold were investigated. The electrical percolation thresholds of the silver nanowires were negatively correlated to the aspect ratio due to their ease of contact with other silver nanowires for the silver nanowires with higher aspect ratio. These results demonstrate the need to control the aspect ratio of silver nanowires in order to maximize their efficient use in electrical applications.

Keywords silver nanowires; aspect ratio; polyol process; percolation

1. Introduction

One-dimensional (1D) metal nanostructures play an important role as both interconnects and active components in fabricating nanoscale electronic devices [1–7]. Among these metal nanostructures, silver nanowires have attracted increasing research attention in the past decade because of their high aspect ratio, and unique electrical, thermal and optical properties, which have supported their potential applications in numerous fields including catalysis, electronics, optoelectronics, sensing, and surface-enhanced spectroscopy [8–12]. Since the properties of 1D silver nanostructure are strongly dependent on their morphology, shapes and aspect ratios, extensive studies on shape- and size-controlled syntheses of silver nanostructures have been carried out [5,6]. The several chemical methods that have been demonstrated to prepare silver nanowires include porous or solid template-directed synthesis, biomimetic synthesis, polyol process, and wet chemical synthesis [13–16]. Among these methods, the polyol process has become widely used as it is an excellent method for the shape- and size-controlled synthesis of silver nanowires. In the polyol process, the morphology of the initial seeds is one of the key factors in generating the silver nanowires. Two types of initial seed are present: single cuboctahedral crystals, and multiple-twinned decahedral particles (MTPs). Silver nanowires with pentagonal cross sections are formed only when the initial seeds are MTPs [3,17]. Thus the structure-controlled synthesis of seeds is useful in the formation of silver nanowires.

The molar ratio between polyvinylpyrrolidone (PVP) and $AgNO_3$ is the other key factor in growth of the silver nanowires. The aspect ratios of silver nanowires strongly depend on

*Address correspondence to Hyoung.-Joon. Jin, Fax: +82-32-865-5178. E-mail: hjjin@inha.ac.kr

the experimental parameters, especially the PVP/$AgNO_3$ molar ratio at a constant $AgNO_3$ concentration [18–20]. Therefore, the PVP amount-controlled synthesis is also useful in the formation of silver nanowires with different aspect ratios. Percolation pathways can easily be formed with a very low load percentage of silver nanowires, leading to considerable reduction of silver loading in comparison with the use of silver nanorods (low aspect ratio). In addition, the electrical percolation threshold of silver nanowires is lower than that of silver nanorods, because the possibility of contact between wires in the adhesive is greater than with rods [1]. Therefore, the longer silver nanowires significantly decrease the percolation threshold in surface conductance.

In this study, we synthesized silver nanowires through a polyol process, with ethylene glycol (EG) as a reducer and solvent and PVP as a capper agent and control agent. The aspect ratio of the silver nanowires was controlled by changing the PVP/$AgNO_3$ molar ratio at a constant $AgNO_3$ concentration. This molar ratio strongly affected the lengths of the silver nanowires. The longest silver nanowires with an average length of 16.46 ± 2.26 μm were synthesized at a PVP/$AgNO_3$ molar ratio of 3 and they facilitated the most rapid formation of a percolation pathway.

2. Experimental

2.1. Materials

Anhydrous ethylene glycol (EG) (99.8%), sodium chloride (NaCl, 99.5%), silver nitrate ($AgNO_3$, 99.9%) and PVP (Mw $\approx$ 55,000) were purchased from Aldrich. All chemicals were used without further purification.

2.2. Synthesis of silver nanowires

Silver nanowires were synthesized by reducing $AgNO_3$ with EG in the presence of PVP. In a typical experimental procedure, 10 ml of 0.1 M $AgNO_3$ solution in EG was heated in a three-necked flask at $\sim$160°C, after which 1 ml of 1.7 mM NaCl solution in EG was added quickly. After reaction for 15 min the seeding step was finished and 0.15 M PVP solution in EG was injected drop-wise into the reaction system by syringes within 10 min. The reaction was kept at $\sim$160°C for another 2 h until the crystal growth step was finished and magnetic stirring was maintained during the entire procedure. After the solution was cooled to room temperature, the final dispersion was diluted with acetone and centrifuged at 4,000 rpm for 30 min. The supernatant dissolved in the residual EG was then removed by syringe and water was added into the centrifuge tube to disperse the products and dissolve the residual PVP. Finally, the supernatant was also removed by syringe, and the process was repeated twice more. These purified products were preserved in ethanol for characterization.

2.3. Characterization

The morphology, diameter and length of the silver nanowires were determined by field emission scanning electron microscopy (FESEM, S-4300, Hitachi, Japan) at an accelerating voltage of 15 kV. Before the analysis, all of the samples were pre-coated with a homogeneous Pt layer through ion sputtering (E-1030, Hitachi, Japan). The crystal structure of the silver nanowires was identified by detecting the peaks of the reduced silver crystals using X-ray diffraction (XRD, DMAX-2500, Rigaku, Japan) by means of a diffractometer with reflection geometry and CuKα radiation (wavelength $\lambda = 0.154$ nm) operated at 40 kV and

100 mA. The data were collected over a scattering angle (2θ) range from 20 to 80°. The electrical conductivity of the uniform films of silver nanowires were measured by using a four-probe method with a high voltage source measurement unit (237 Keithley)

3. Results and discussion

3.1 Influence of seeding time and reaction temperature

In the polyol process, the morphology of the initial seeds is one of the key factors in generating silver nanowires. The two types of initial seeds, MTPs and single-crystal seeds, form nanowires and nanoparticles, respectively. It has been suggested that the two formation mechanisms are thermodynamically controlled and kinetically controlled, respectively [3]. Therefore, the synthesis of silver nanowires is favored by using MTPs with a thermodynamically stable structure as the initial seed. Consequently, we studied the influence of seeding time and reaction temperature on the expansion of the amount of MTPs in the seeds and nanowires in the final products.

First, the seeding time was shown to play an important role in the formation of silver nanowires. Figure 1 shows SEM images of the synthesized products obtained by a standard process with two different seeding times. Silver nanoparticles were formed at an insufficient seeding time of 5 min, as shown in figure 1(A). However, silver nanowires were formed at a longer seeding time of 15 min, as shown in figure 1(B). In general, shorter and longer reaction times favor kinetic control and thermodynamic reaction control, respectively. Therefore, a short seeding time generated silver nanoparticles due to the presence of numerous kinetically controlled, single crystals. In contrast, silver nanowires were the principle final product, because the thermodynamically controlled MTPs were mainly formed at sufficient seeding time.

Second, the reaction temperature was shown to control the morphology of the final product. Figure 2 shows SEM images of silver products synthesized at three different reaction temperatures. At the lower reaction temperature of 120°C, silver nanoparticles were the principle products, as shown in figure 2(A). But, when the reaction temperature rose to 160°C, nanowires were the principal product, as shown in figure 1(B). When the reaction temperature was further increased to 180°C, the principle products remained silver nanowires, as shown in figure 2(B). This influence of reaction temperature on the product morphology is also related to the activation energy of the seed formation. The relatively low

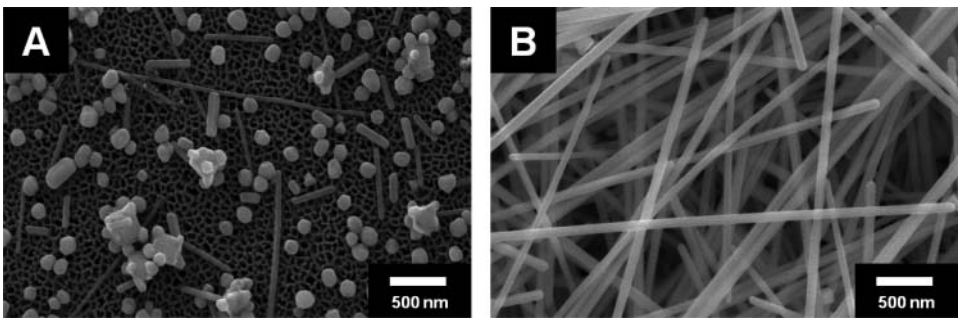

Figure 1. SEM images of synthesized silver nanowires with two different seeding times: (A) 5 min, and (B) 15 min.

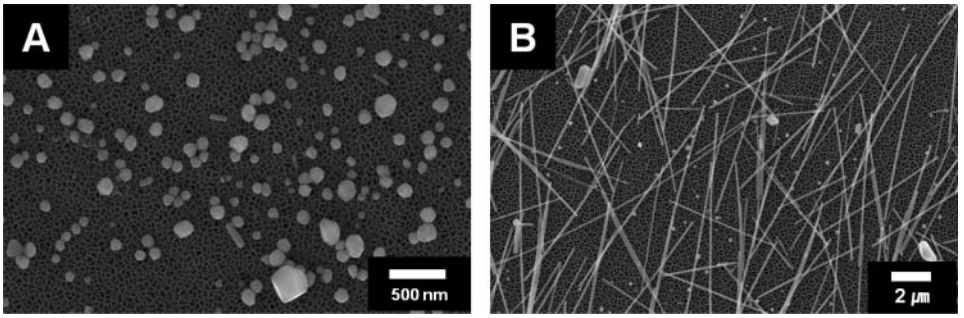

Figure 2. SEM images of synthesized silver nanowires with two different reaction temperatures: (A) 120°C, and (B) 180°C.

reaction temperature cannot supply enough energy required for the MTP formation because the energy required is higher than that of single crystals. Conversely, silver nanowires are formed as the final product when the reaction temperature is raised over 160°C because the energy required for MTP formation is enough. To summarize, MTP formation required a relatively high temperature of 160°C, which was appropriate for synthesis of silver nanowires.

3.2 Influence of the PVP/$AgNO_3$ molar ratio

The aspect ratios of the silver nanowires differed according to the PVP/$AgNO_3$ molar ratio. Figure 3 shows SEM images of the silver nanowires prepared at PVP/$AgNO_3$ molar

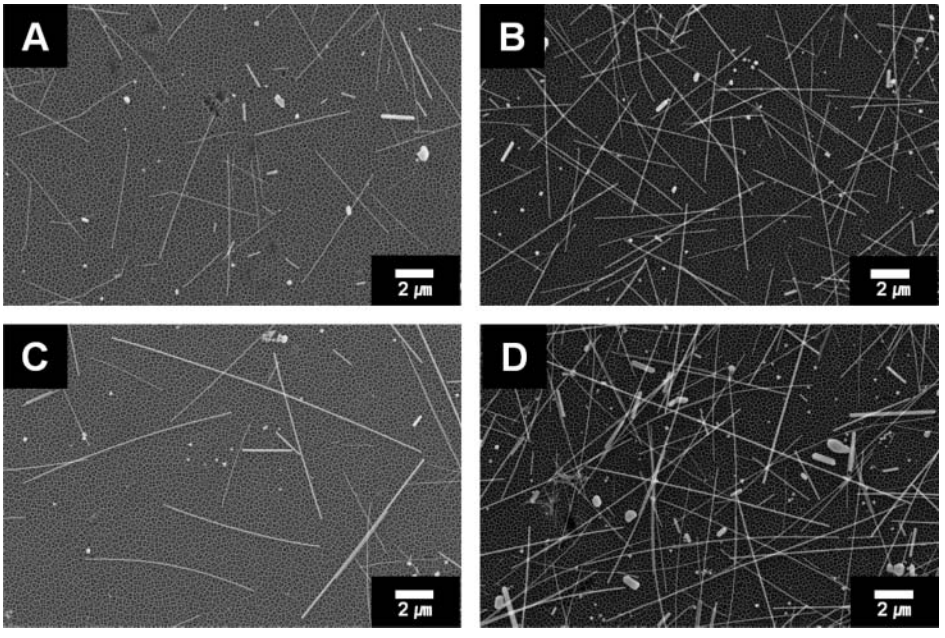

Figure 3. SEM images of silver nanowires obtained with different molar ratios between the repeating unit of PVP (Mw = 55,000, n = 500) and $AgNO_3$ (PVP/$AgNO_3$): (A) 0.75, (B) 1.5, (C) 2.25, and (D) 3.

Table 1. Average Length and Diameter of the Silver Nanowires Obtained at Four Different Molar Ratios Between the Repeating Unit of PVP and $AgNO_3$

The molar ratios	Length (μm)	Diameter (nm)	Aspect ratio
0.75	4.2 ± 2.9	73 ± 3	58 ± 4
1.5	6.1 ± 2.9	77 ± 2	80 ± 4
2.25	11.3 ± 7.1	78 ± 4	144 ± 9
3	16.5 ± 2.3	78 ± 4	210 ± 6

*n = 100.

ratios of 0.75, 1.5, 2.25 and 3. The average length of the silver nanowires increased with increasing molar ratio. Table 1 lists the corresponding average length, diameter and aspect ratio. MTP seeds grow into silver nanowires by Ostwald ripening and chemical bonding between PVP and silver as the small silver nanoparticles spontaneously agglomerate into larger ones (Ostwald ripening) and the {111} facet of the seed remains active due to the markedly stronger chemical bonding between PVP and {100} compared to that between PVP and {111} [7,21]. Short silver nanowires were produced at relatively low PVP/$AgNO_3$ molar ratio because PVP could not effectively passivate the side surfaces of individual nanowires, resulting in the formation of short silver nanowires [22]. However, due to the sufficient PVP supply for interaction with silver at relatively high PVP/$AgNO_3$ molar ratio, long silver nanowires were formed. However, as the PVP/$AgNO_3$ molar ratio was increased above 3, only silver nanoparticles were obtained due to the formation of a thick coating of PVP on all faces of the seeds and its effect in reducing the selectivity in interaction between PVP and Ag.

Figure 4 shows the XRD patterns of the silver nanowires, and the peaks at 38.1°, 44.3°, 64.4°, and 77.8° were indexed as the {111}, {200}, {220}, and {311} facets of the face-centered-cubic phase of silver belonging to the space group Fm3m [255] (JCPDS file No. 04–0783). The {111} and {200} facets, which arose dominantly from the ends and the body of the silver nanowires, respectively, were noticeable diffraction peaks. Table 2 shows that the intensity ratios between the {111} and {100} facets were relatively higher than the theoretical ratio of 2.5, which was attributed to the anisotropic growth of the as-synthesized silver nanowires [23]. In addition, the intensity ratio between the {111} and {100} facets increased with increasing PVP amount, indicating that the aspect ratios of the silver nanowires can be controlled according to the PVP/$AgNO_3$ molar ratio.

Table 2. Intensity Ratios Between the {111} and {100} Facets at Four Different PVP/$AgNO_3$ Molar Ratios

PVP/$AgNO_3$ molar ratios	The ratio of the intensity between the {111} and {100} facets
0.75	2.4
1.5	2.6
2.25	3.0
3	3.3

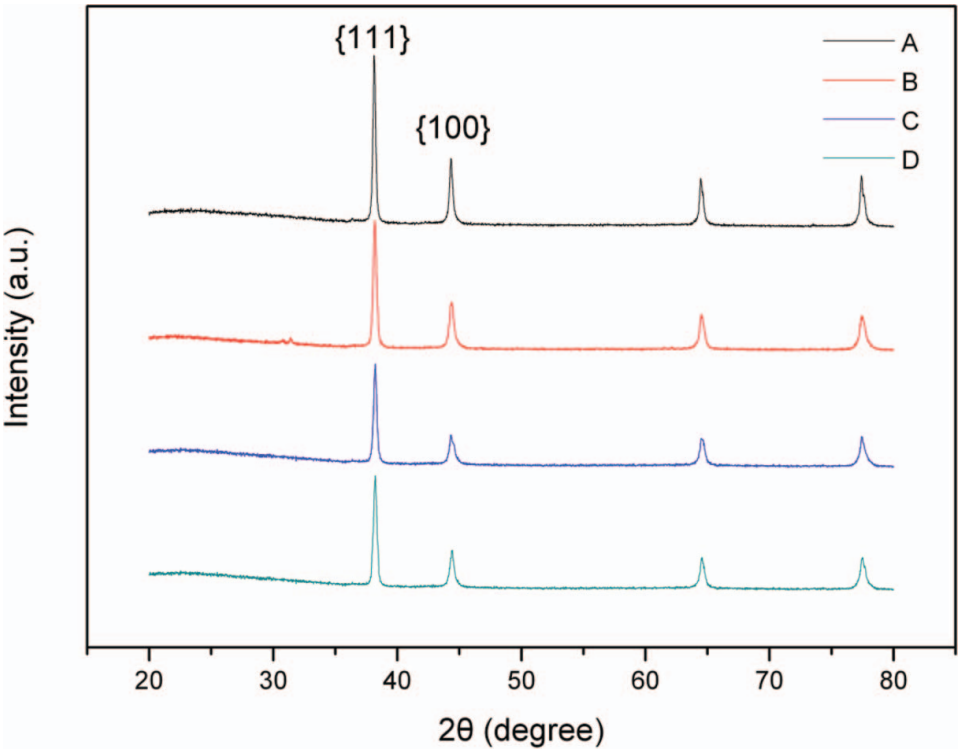

Figure 4. XRD patterns of the silver nanowires according to the PVP/$AgNO_3$ molar ratio: (A) 0.75, (B) 1.5, (C) 2.25, and (D) 3.

Figure 5 shows a schematic illustration outlining the mechanism for the formation of morphology-controlled silver seeds and the growth of silver nanostructures from these seeds in the presence of PVP. The creation of single crystal seeds is favored by a low reaction temperature and a short seeding time (step a in figure 5), and that of MTPs by a high reaction temperature and a long seeding time (step b in figure 5), leading to the

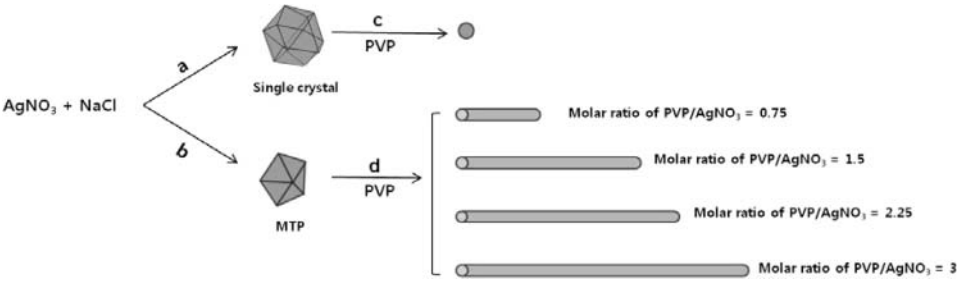

Figure 5. Schematic illustration of the experimental mechanisms that generated silver nanostructures: (a) formation of MTPs with thermodynamic stability, (b) formation of single crystal seeds with kinetic stability, (c) isotropic growth directed by unselective adsorption of PVP on the surface of seeds, resulting in nanoparticles, and (d) anisotropic growth directed by selective adsorption of PVP on the surface of seeds, resulting in silver nanowires.

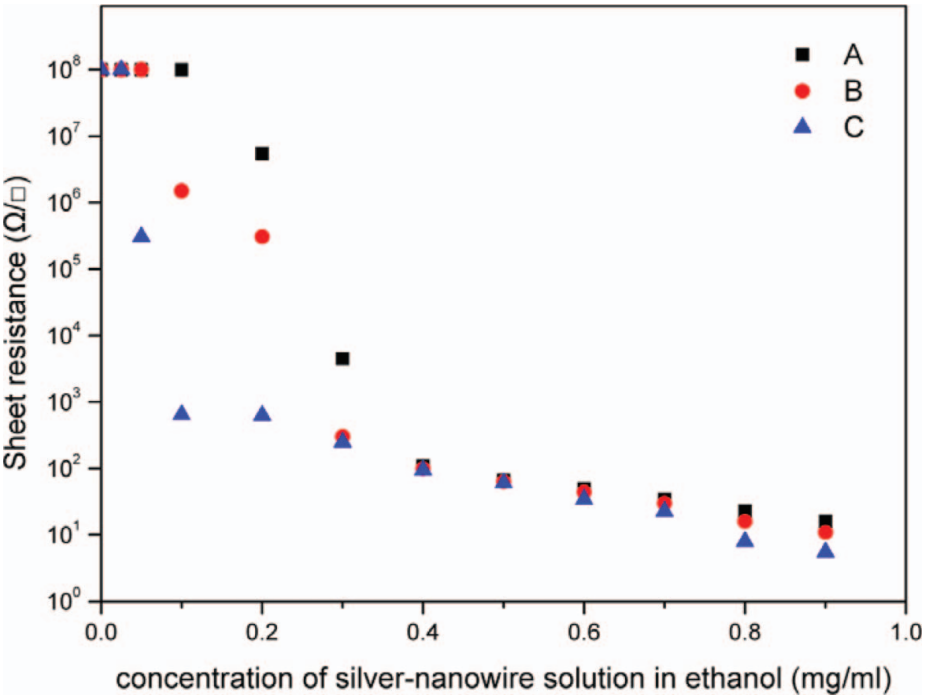

Figure 6. Sheet resistance of the silver nanowire films with the aspect ratio controlled by using different PVP/$AgNO_3$ ratios of (A) 1.5, (B) 2.25, and (C) 3.

formation of silver nanoparticles (step c in figure 5) and silver nanowires, respectively. In this study, we propose a method for controlling the aspect ratio of silver nanowires, as shown in step d in figure 5. Because of the insufficient PVP supply for passivating the side surfaces of the silver nanowires at a low PVP/$AgNO_3$ molar ratio, compared to that at a higher PVP/$AgNO_3$ molar ratio, longer silver nanowires were synthesized.

3.3 Conductive percolation

Figure 6 shows the percolation behavior, which explains the effects of the aspect ratio of the silver nanowires on the conductivity of the silver nanowire film. To produce uniform films of silver nanowires, we used a vacuum filtration method comprising vacuum filtering of a dilute suspension of nanowires in a solvent over a porous alumina filtration membrane (Whatman, 20 nm pore size, 47 mm diameter). The higher aspect ratio silver nanowires with a PVP/$AgNO_3$ molar ratio of 3 showed a lower electrical percolation threshold due to their ease of contact with other silver nanowires. In the lower aspect ratio silver nanowires with a PVP/$AgNO_3$ molar ratio of 1.5, many more silver nanowires were required to reach the electrical percolation threshold than in high aspect ratio ones.

4. Conclusions

We synthesized silver nanowires through a polyol process, with EG as a reducer and solvent and PVP as a capper agent and control agent. We examined the effects of changing the

synthesis conditions of seeding time, reaction temperature and PVP/$AgNO_3$ molar ratio because the two key factors in the synthesis of silver nanowires were the morphology of the initial seeds and the PVP/$AgNO_3$ molar ratio as they strongly affected the aspect ratio of silver nanowires. The high aspect ratio silver nanowires exhibited a low electrical percolation threshold due to their ease of contact with other silver nanowires. Therefore, such high aspect ratio silver nanowires can be applied to electronic devices, especially transparent electrodes, due to their high conductivity and low load percentage of silver nanowires (high aspect ratio) in comparison with the use of silver nanoparticles and nanorods (low aspect ratio).

Acknowledgements

This research was supported by Basic Science Research Program through the National Research Foundation of Korea (NRF) funded by the Ministry of Education, Science and Technology (2011–0009614).

References

[1] Sun, Y. (2010). *Nanoscale*, *2*, 1626.
[2] Chen, C., Wang, L., Jiang, G., Zhou, J., Chen, X., Yu, H., & Yang, Q. (2006). *Nanotechnology*, *17*, 3933.
[3] Chen, C., Wang, L., Jiang, G., Yang, Q., Wang, J., Yu, H., Chen, T., Wang, C., & Chen, X. (2006). *Nanotechnology*, *17*, 466.
[4] Sun, Y., Gates, B., Mayers, B., & Xia, Y. (2002). *Nano Lett.*, *2*, 165.
[5] Tsuji, M., Matsumoto, K., Miyamae, N., Tsuji, T., & Zhang, X. (2007). *Crystal growth & design*, *7*, 311.
[6] Gao, Y., Jiang, P., Liu, D., Yuan, H., Yan, X., Zhou, Z., Wang, J., Song, L., Liu, L., & Zhou, W. (2004). *J. Phys. Chem. B*, *108*, 12877.
[7] Sun, Y., Yin, Y., Mayers, B. T., Herricks, T., & Xia, Y. (2002). *Chem. Mater.*, *14*, 4736.
[8] Pestryakov, A. N., Bogdanchikova, N., & Knop-Gericke, A. (2004). *Catalysis Today*, *91*, 49.
[9] Hu, L., Kim, H. S., Lee, J. Y., Peumans, P., & Cui, Y. (2010). *ACS nano*, *4*, 2955.
[10] Jin, R., Cao, Y. W., Mirkin, C. A., Kelly, K., Schatz, G. C., & Zheng, J. (2001). *Science*, *294*, 1901.
[11] McAlpine, M. C., Ahmad, H., Wang, D., & Heath, J. R. (2007). *Nature Materials*, *6*, 379.
[12] Aroca, R. F., Goulet, P. J. G., dos Santos Jr, D. S., Alvarez-Puebla, R. A., & Oliveira Jr, O. N. (2005). *Anal. Chem.*, *77*, 378.
[13] Tsuji, M., Hashimoto, M., Nishizawa, Y., Kubokawa, M., & Tsuji, T. (2005). *Chem. Eur. J.*, *11*, 440.
[14] Luu, Q. N., Doorn, J. M., Berry, M. T., Jiang, C., Lin, C., & May, P. S. (2011). *Journal of colloid and interface science*, *356*, 151.
[15] Sun, Y., Mayers, B., Herricks, T., & Xia, Y. (2003). *Nano Lett.*, *3*, 955.
[16] Jiang, Z. Y., Xie, Z. X., Zhang, S. H., Xie, S. Y., Huang, R. B., & Zheng, L. S. (2003). *Chemical physics letters*, *374*, 645.
[17] Yan, H., Park, S. H., Finkelstein, G., Reif, J. H., & LaBean, T. H. (2003). *Science*, *301*, 1882.
[18] Gao, Y., Jiang, P., Song, L., Liu, L., Yan, X., Zhou, Z., Liu, D., Wang, J., Yuan, H., & Zhang, Z. (2005). *J. Phys. D: Appl. Phys.*, *38*, 1061.
[19] Wei, G., Nan, C. W., Deng, Y., & Lin, Y. H. (2003). *Chem. Mater.*, *15*, 4436.
[20] Sun, Y., & Xia, Y. (2002). *Science*, *298*, 2176.
[21] Caswell, K., Bender, C. M., & Murphy, C. J. (2003). *Nano Lett.*, *3*, 667.
[22] Gou, L., Chipara, M., & Zaleski, J. M. (2007). *Chem. Mater.*, *19*, 1755.
[23] Wiley, B., Sun, Y., Mayers, B., & Xia, Y. (2005). *Chem. Eur. J.*, *11*, 454.